Irreversible Electroporation: Just Another Form of Thermal Therapy?

Martin J. C. van Gemert,[1]* Peter G. K. Wagstaff,[2] Daniel M. de Bruin,[1,2] Ton G. van Leeuwen,[1] Allard C. van der Wal,[3] Michal Heger,[4] and Cees W. M. van der Geld[5]

[1]*Department of Biomedical Engineering & Physics, Academic Medical Center, University of Amsterdam, Amsterdam, The Netherlands*
[2]*Department of Urology, Academic Medical Center, University of Amsterdam, Amsterdam, The Netherlands*
[3]*Department of Pathology, Academic Medical Center, University of Amsterdam, Amsterdam, The Netherlands*
[4]*Department of Experimental Surgery, Academic Medical Center, University of Amsterdam, Amsterdam, The Netherlands*
[5]*Department of Mechanical Engineering, Eindhoven University of Technology, Eindhoven, The Netherlands*

BACKGROUND. Irreversible electroporation (IRE) is (virtually) always called non-thermal despite many reports showing that significant Joule heating occurs. Our first aim is to validate with mathematical simulations that IRE as *currently practiced* has a non-negligible *thermal* response. Our second aim is to present a method that allows simple temperature estimation to aid IRE treatment planning.

METHODS. We derived an approximate analytical solution of the bio-heat equation for multiple 2-needle IRE pulses in an electrically conducting medium, with and without a blood vessel, and incorporated published observations that an electric pulse increases the medium's electric conductance.

RESULTS. IRE simulation in prostate-resembling tissue shows thermal lesions with 67–92°C temperatures, which match the positions of the coagulative necrotic lesions seen in an experimental study. Simulation of IRE around a blood vessel when blood flow removes the heated blood between pulses confirms clinical observations that the perivascular tissue is thermally injured without affecting vascular patency.

CONCLUSIONS. The demonstration that significant Joule heating surrounds current multiple-pulsed IRE practice may contribute to future in-depth discussions on this thermal issue. This is an important subject because it has long been under-exposed in literature. Its awareness pleads for preventing IRE from calling "non-thermal" in future publications, in order to provide IRE-users with the most accurate information possible. The prospect of thermal treatment planning as outlined in this paper likely aids to the important further successful dissemination of IRE in interventional medicine. *Prostate 75:332–335, 2015.*

INTRODUCTION

Irreversible electroporation (IRE) is (virtually) always called *non-thermal* [1,2], despite many reports showing that significant Joule heating occurs, that is, by mathematical modeling (e.g., [3]), from measured temperatures that irreversibly injure tissues [4] and by histology showing coagulative necrosis in IRE-affected regions (e.g., [1,2,4–6]). The classification "*non-thermal*" suggests that IRE at any setting induces cell death without the danger of Joule heating which make IRE

Conflicts of Interest: None.

*Correspondence to: Prof. Martin J. C. van Gemert, PhD, Department of Biomedical Engineering & Physics, Academic Medical Center, Amsterdam, The Netherlands.
E-mail: m.j.vangemert@amc.uva.nl
Received 9 July 2014; Accepted 29 August 2014
DOI 10.1002/pros.22913
Published online 18 October 2014 in Wiley Online Library (wileyonlinelibrary.com).

procedures prone to serious thermal-related complications. Our first aim is therefore to validate with mathematical simulations that *currently practiced* IRE, in this paper comprising 1.5 or 2 kV over a needle-pair of 1 cm distance, 100 pulses of 0.1 ms duration per pulse and 1 Hz repetition frequency, has a non-negligible *thermal* response. Our second aim is to present a method that allows simple thermal treatment planning of IRE procedures. To achieve these goals, we will mathematically simulate the temperature response of multiple pulsed 2-needle IRE by (1) deriving an approximate analytical solution of the bio-heat equation for this IRE configuration in an electrically conducting medium, with and without a blood vessel, and (2) incorporating published observations that an electric pulse increases the medium's electric conductance. Finally, we compare the simulations with literature results.

METHOD

IRE Case 1: Tissue

We adopt the electric field distribution, E (kV/cm), as calculated by Davalos and Rubinsky [3] for 2 kV over a 1 cm needle distance. Their Figure 3B gives the resulting temperatures, ΔT_{max}, at the end of an electric pulse of $\Delta t = 0.51$ ms in tissue with an electric conductance of $\sigma_0 = 0.2$ S/m from $\Delta T_{max}(r,\Delta t) = (\sigma_0 E(r)^2/\rho c) \times \Delta t$, with radial coordinate r, mass density $\rho \approx 10^3$ (kg/m^3) and heat capacity $c \approx 3.5 \times 10^3$ (J/kg/°C). The essence of our method is that we approximate ΔT_{max} by a Gaussian radial function and determine its 1/e-value at $r = r_0$. With these two parameters the bio-heat Equation (1) below can be analytically solved, also for $t \gg \Delta t$. The $\Delta T_{max}(r,\Delta t)$ curve of Figure 3B of [3] fits well as $\Delta T_{max}(r,0.51) \approx \Delta T_0 \exp(-1.4 \cdot r^2)$, with $\Delta T_0 = 21$°C and $r_0 = 0.85$ mm, from fitting ΔT_{max} at $r = 0.5$ and 0.828 mm. In our simulations we use 0.1 ms and 0.3 S/m (for prostate tissue [1]), so $\Delta T_0 = 6.28$°C for 2 kV and 3.53°C for 1.5 kV. Further, σ_0 increases during each IRE pulse [7] and the top of the peaks of Figure 4 of [7] fitted well to $\sigma_n/\sigma_0 \approx 1.29\sqrt{0.36\sqrt{n}+1}$. At longer times, $\Delta T(r,t)$ follows from the solution of the bio-heat equation, which conserves the volumetric rates of heat produced by E and removed by thermal conduction. Ignoring heat loss by tissue perfusion [3], it is

$$\frac{\partial \Delta T(r,t)}{\partial t} = \frac{\sigma E(r)^2}{\rho c} + \alpha \nabla^2 \Delta T(r,t) \qquad (1)$$

with thermal diffusivity $\alpha \approx 0.13$ mm^2/s and 2nd order differential (Laplace) operator ∇^2(m^{-2}). Equation (1) has no simple general analytical solution. However, the Gaussian profile defined above may be thought to originate from radial cooling of an "instantaneous line source of heat" ([8], Equation (1) of page 258) during time period $\tau = r_0^2/4\alpha \approx 1.4$ sec, where τ is the time constant for heat conduction. Then, a short IRE pulse at $t = 0$ has the simple thermal analytical solution to Equation (1) of

$$\Delta T(r,t) \approx \Delta T_0 \frac{\exp[-(r/r_0)^2/\{1+t/\tau\}]}{1+t/(\tau)} \equiv \Delta T_0 F(r,t) \qquad (2)$$

Equation (1) is linear in ΔT so ΔT-responses to multiple pulses can be added as follows. We use that the 1st pulse, at $t = 0$, yields $\Delta T^1(r,0) = \Delta T_0 F^1(r,0)\sigma_1/\sigma_0$. Just after the 2nd pulse, say 1 sec later, the 1st pulse reduced to $\Delta T^1(r,1) = \Delta T_0 F^1(r,1)\sigma_1/\sigma_0$. The 2nd pulse gives $\Delta T^2(r,1) \equiv \Delta T_0 F^1(r,0)\sigma_2/\sigma_0$, thus proportional to the response of the 1st pulse at $t = 0$. Two pulses, at $t = 1$ sec, thus cause $\Delta T^2(r,1) = \Delta T_0[F^1(r,0)\sigma_2/\sigma_0 + F^1(r,1)\sigma_1/\sigma_0]$, that is, including the two responses to the *first* pulse at the two pulse events. Similarly, three pulses, at $t = 2$ sec, give $\Delta T(r,2) = \Delta T_0[F^1(r,0)\sigma_3/\sigma_0 + F^1(r,1)\sigma_2/\sigma_0 + F^1(r,2)\sigma_1/\sigma_0]$. Writing this as $\Delta T(r,2) = \Delta T_0 \sum_{n=0}^{3-1} F^1(r,n)\sigma_{3-n}/\sigma_0$, using Equation (2) and including pulse rate f (Hz), approximately solves Equation (1) analytically following N consecutive pulses, at $t = (N-1)f^{-1}$ sec, as

$$\begin{aligned}\Delta T(r(N-1)f^{-1}) &\approx \Delta T_0 \sum_{n=0}^{N-1} \frac{\exp[-(r/r_0)^2/(1+\{nf^{-1}/(\tau)\})]}{1+\{nf^{-1}/(\tau)\}} \\ &\times \left(1.29\sqrt{0.36\sqrt{(N-n)}+1}\right)\end{aligned} \qquad (3)$$

IRE Case 2: Tissue With (Large) Blood Vessel

Two-needle IRE around a blood vessel can be simulated if blood flow removes the heated blood between pulses, keeping the intima at 37°C. An analytical solution to Equation (1) is available if radial cooling of the vessel wall is approximated by 1-D diffusion in the x-direction (intima at $x = 0$, Fig. 1), implying that the perivascular tissue becomes a 1-D semi-infinite medium. Using [8], Equation (1) of page 85, and that each pulse increases the whole perivascular tissue by ΔT_0 °C, solves Equation (1) as $\Delta T(x,t) = \Delta T_0 \mathrm{erf}(x/\sqrt{4\alpha t})$. Thus, as Equation (3), an approximate solution of Equation (1) following N consecutive pulses, at $t = (N-1)f^{-1}$ sec, is

$$\begin{aligned}\Delta T(x(N-1)f^{-1}) &\approx \Delta T_0 \sum_{n=0}^{N-1} \mathrm{erf}\left(x/\sqrt{4\alpha n f^{-1}}\right) \\ &\times \left(1.29\sqrt{0.36\sqrt{(N-n)}+1}\right)\end{aligned} \qquad (4)$$

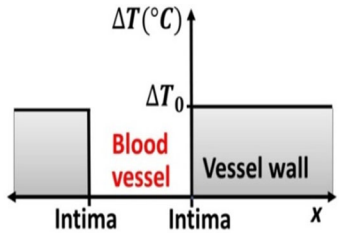

Fig. 1. IRE around a blood vessel and 1-D heat conduction in the x-direction. The needles are assumed to be placed at 5 mm from the "center of the blood vessel."

RESULTS

Figure 2 shows simulations for f = 1 Hz.

IRE Case 1

For prostate tissue, 1.5 kV over 1 cm, $\Delta t = 0.1$ ms, N = 100 [1], a temperature of 92°C occurs at the needle-tissue boundary (curve 1), which falls to 80°C at r = 1 mm (curve 2) and 56°C at r = 3 mm (curve 3a). However, at r = 3 mm, the Gaussian fit used gives $\Delta T_{max} \approx 0$ rather than ≈0.55°C which results in an 11°C underestimated temperature at N = 100, thus a better value than 56°C is 67°C (curve 3b), based on

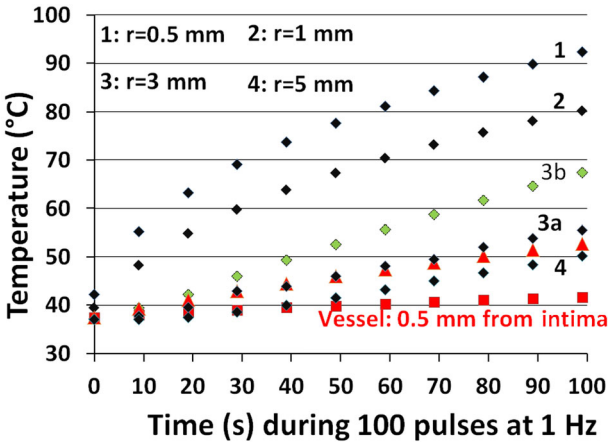

Fig. 2. Simulated temperatures, Equation (3), of 100 pulses of 2-needle IRE, for 1.5 kV over 1 cm distance, $\Delta t = 0.1$ ms, at 1 Hz, for prostate-resembling tissue [1] without (curves 1, 2, 3a, 3b, 4) and with a blood vessel, Equation (4), for 2 kV (red symbols). Curves 1, 2, 3a, 4 have been computed by fitting Figure 3B of [3] at radii 0.5 and 0.828 mm, and curve 3b by fitting two Gaussian functions at radii 0.5 and 0.828 mm (1st Gaussian) and 2 and 5 mm (2nd Gaussian), converted as before to 1.5 kV, $\Delta t = 0.1$ ms, and $\sigma_0 = 0.3$ S/m, as: $\Delta T_{max} = 3.86 \cdot \exp\ [-(r/0.603)^2] + 0.215 \cdot \exp\ [-(r/3.892)^2]$. Curves 1, 2, and 4 do not change much when using two Gaussians compared to one. The red triangles between curves 3a and 4 represent the curve "Vessel: 2 mm from intima."

including two Gaussian functions for ΔT_{max} (defined in the caption of Fig. 2). Coordinate r = 3 mm matches the position of the lesion margin shown in Figure 4 of [1], implying that these pathology-assessed coagulative necrotic lesions are thermal injuries that correspond with our computed temperatures of 67–92°C.

IRE Case 2

For a (large) blood vessel at r = 5 mm, 2 kV over the needles, $\Delta T_0 \approx 0.15$°C (from $\Delta T_0 \approx 0.5$°C in Figure 3B of [3]), we simulate a temperature of 41°C close to the intima but 53°C at 2 mm from the intima (thus at r = 3 mm). We neglected the extra ≈0.5°C shown in Figure 3B of [3] at r = 3 mm which would have added another ≈10°C. In our opinion, this explains for the first time why IRE of blood vessels is effective and safe [6]. It suggests a clinical role for matching the measured blood flow with the IRE pulse frequency.

DISCUSSION

The message of this paper is that although one single IRE pulse may raise the temperature a few degrees only, 100 consecutive pulses can produce temperatures that easily injure tissues irreversibly. From that standpoint, IRE is not different from other Joule heating-based therapies. Particularly, tissues of large electric conductance warrant caution during IRE, for example, urine (1.9 S/m [9]) within the renal collecting system and bile ducts when filled with bile (1.27 S/m [9]).

To the best of our knowledge, we are the first to analytically solve, albeit approximately, the temperature response to multiple-pulsed IRE by fitting the electric field distribution to a Gaussian function. The linearity of Equation (1) in ΔT obviously allows this approach to be extended to the use of more than just one Gaussian (see curve 3b of Fig. 2 for two Gaussians). Thermal treatment planning becomes simple now, based on Equation (3), and can conceptually be extended to multiple-needle IRE geometries with programmed activation of the various needle-pairs. Treatment planning before—as well as temperature measurements during—IRE oncologic procedures are particularly important because insufficient thermal effects at the boundaries of treated lesions are notorious for causing tumor recurrence.

Compared to the numerical analysis in [10], we achieved very similar results, for example, the first two T-peaks of their Figure 5, that is, T ≈ 33.8 and ≈34°C in response to 40 pulses of 0.5 kV over 0.5 cm and 0.05 ms, in sets of 20 separated by 3.5 sec, versus our estimates of ≈33.7 and 34.2°C. Further, the literature gives thermal evaluations of 2-plate and

multiple-needle IRE. The former has negligible heat conduction during multiple pulses, the latter likely gives slightly higher temperatures compared to 2-needle IRE. As an example, Faroja et al. [4] measured temperatures as high as 84°C of 2-plate IRE (their Table 1) in in vivo porcine liver, using 2.5 kV over a 1 cm plate distance and 360 pulses of 0.1 ms at 1 Hz. For 40 and 90 pulses at 2.5 kV they found $\Delta T \approx 11$ and 18°C. Using $\Delta T = \sum_{n-1}^{N} (\sigma_n E^2/\rho c)\Delta t$ and $\sigma_0 \approx 0.09$ S/m for liver [9], gave $\Delta T \approx 15$ and 39°C.

Also, non-thermal IRE effects have been documented, for example, by Gehl et al. (Fig. 3 of [11]), using 2-plate IRE around the tibia of mice, eight pulses at 0.2–1.4 kV/cm and Δt of 10–2,000 μs. These authors described perfusion delays of 200–1,800 sec, which they attributed to sympathetic nerve-mediated reflexory vasoconstriction of afferent arterioles, characterized as a Raynaud-like phenomenon and comparable to ST depression observed in the ECG of patients following atrial defibrillation. The reported perfusion delays correspond to simulated temperature increases of 2–33°C.

The thermal nature of IRE may actually have several important therapeutic consequences in terms of cancer treatment. As described in [12], exposure of cancer cells to IRE induces necrotic [1,2,4–6] and possibly apoptotic and/or autophagic cell death. Any of these forms of cell death activates the immune system through sterile inflammation [13], leading to debridement of necrotic tissue followed by tissue remodeling. It is also likely that the adaptive immune system elicits an anti-tumor immune response against residual, viable cancer cells in the treated volume as well as distal, non-treated cancer cells [14].

CONCLUSION

The demonstration that significant thermal effects at current IRE settings cannot be ignored hopefully contributes to future in-depth discussions on thermal issues that surround IRE. This is an important subject because it has long been under-exposed in literature. Such a discussion adds to safer and more precisely planned IRE procedures. The thermal nature of current IRE practice pleads for preventing IRE from calling "non-thermal" in future publications, in order to provide IRE-users with the most accurate information possible. The prospect of treatment planning as outlined above may aid to the important further successful dissemination of IRE in interventional medicine.

REFERENCES

1. Neil RE, Millar JL, Kavnoudias H, Royce P, Rosenfeldt F, Pham A, Smith R, Davalos RV, Thomson KR. In vivo characterization and numerical simulation of prostate properties for non-thermal irreversible electroporation ablation. Prostate 2014;74: 458–469.
2. Golberg A, Yarmush ML. Nonthermal irreversible electroporation: Fundamentals, applications and challenges. IEEE Trans Biomed Eng 2013;60:707–714.
3. Davalos RV, Rubinsky B. Temperature considerations during irreversible electroporation. Int J Heat Mass Transfer 2008;51: 5617–5622.
4. Faroja M, Ahmed M, Applebaum L, Ben-David E, Moussa M, Sosna J, Nissenbaum I, Goldberg SN. Irreversible electroporation ablation: Is all the damage nonthermal? Radiology 2013;266: 462–470.
5. Appelbaum L, Ben-David E, Faroja M, Nissenbaum Y, Sosna J, Goldberg SN. Irreversible electroporation ablation: Creation of large-volume ablation zones in in vivo porcine liver with four-electrode arrays. Radiology 2014;270:418–424.
6. Lee EW, Chen C, Prieto VE, Dry SM, Loh CT, Kee ST. Advanced hepatic ablation technique for creating cell death: Irreversible electroporation. Radiology 2010;255:426–433.
7. Ivorra A, Al-Sakere B, Rubinsky B, Mir LM. In vivo electrical conductivity measurements during and after tumor electroporation: Conductivity changes reflect the treatment outcome. Phys Med Biol 2009;54:5949–5963.
8. Carslaw HS, Jaeger JC. Conduction of heat in solids. 2nd ed. Oxford: Clarendon Press; 1986.
9. Gabriel C, Peyman A, Grant EH. Electrical conductivity of tissue at frequencies below 1 MHz. Phys Med Biol 2009;54:4863–4878.
10. Garcia PA, Rossmeisl JH, Neil RE, Ellis TL, Davalos RV. A parametric study delineating irreversible electroporation from thermal damage based on a minimally invasive intracranial procedure. Biomed Eng Online 2011;10:34 (1–21).
11. Gehl J, Skovsgaard T, Mir LM. Vascular reactions to in vivo electroporation: Characterization and consequences for drug and gene delivery. Biochim Biophys Acta 2002;1569:51–58.
12. Heger M, van Golen RF, Broekgaarden M, van den Bos RR, Neumann HAM, van Gulik TM, van Gemert MJC. Endovascular laser-tissue interactions and biological responses in relation to endovenous laser therapy. Lasers Med Sci 2014;26:405–422.
13. Hirsiger S, Simmen HP, Werner CM, Wanner GA, Rittirsch D. Danger signals activating the immune response after trauma. Mediators Inflamm 2012;2012:315941.
14. Thong PS, Ong KW, Goh NS, Kho KW, Manivasager V, Bhuvaneswari R, Olivo M, Soo KC. Photodynamic-therapy-activated immune response against distant untreated tumours in recurrent angiosarcoma. Lancet Oncol 2007;8:950–952.